Original Article

ADAM10/17-Dependent Release of Soluble c-Met Correlates with Hepatocellular Damage

(c-Met / HGF / shedding / ADAM metalloproteinase / liver / cholangitis)

K. CHALUPSKÝ[1], I. KANCHEV[1], O. ŽBODÁKOVÁ[1], H. BURYOVÁ[1], M. JIROUŠKOVÁ[1], V. KOŘÍNEK[2], M. GREGOR[1], R. SEDLÁČEK[1]

[1]Laboratory of Transgenic Models of Diseases, [2]Laboratory of Cell and Developmental Biology, Institute of Molecular Genetics of the ASCR, v. v. i., Prague, Czech Republic

Abstract. The signalling pathway elicited by hepatocyte growth factor (HGF) and its receptor c-Met is indispensable for liver development and regeneration. It has been described that c-Met is released from the cell surface by a disintegrin and metalloprotease 10 (ADAM10) resulting in a soluble c-Met form known as sMet. Using the human hepatocellular HepG2 and hepatic stellate cell LX2 lines we show that sMet is released from the cell surface of liver cells by both ADAM17 and ADAM10, with ADAM17 appearing to be the major proteinase. Moreover, using a mouse model of 3,5-diethoxycarbonyl-1,4-dihydroxycollidine (DDC)-induced hepatobiliary obstruction we show that serum levels of sMet correlate well with the liver damage state and consecutive regeneration as well as with established markers of liver damage such as alanine aminotransferase (ALT), aspartate transaminase (AST), alkaline phosphatase (ALP), and total bilirubin. However, sMet exhibited remarkably better correlation with liver damage and inflammation than did serum tumour necrosis factor α (TNF-α), whose shedding is also mediated by ADAM proteolytic activity. Our results indicate that the proteolytic activity of ADAM10/17 is essential for regulating HGF/c-Met signalling during acute liver damage and following regeneration and that the differential serum levels of sMet together with expression of c-Met/HGF might be a useful indicator not only for damage, but also for ongoing liver regeneration.

Introduction

c-Met is a class I transmembrane tyrosine kinase known to be the only receptor for HGF that is produced by stromal cells in the liver (Birchmeier et al., 2003; Ma et al., 2003). HGF/c-Met signalling does not appear to play a significant role in liver homeostasis under normal physiologic conditions, but is essential for liver development and regeneration following hepatic injury (Uehara et al., 1995; Comoglio, 2001; Huh et al., 2004). The mature receptor is composed of a 50 kDa α ligand-binding subunit and a 145 kDa β subunit whose cytosolic domain is responsible for tyrosine kinase activity (Giordano et al., 1988; Ma et al., 2003). The signalling pathways downstream of c-Met are well described, involving many scaffolding adaptors and surface signal modifiers; the three major c-Met-dependent pathways include the mitogen-activated protein kinase (MAPK) pathway, the phosphatidylinositol 3-kinase (PI3K)-Akt axis, and the STAT pathway (Trusolino et al., 2010). These c-Met-dependent signalling pathways are essential for liver regeneration initiated in response to acute and chronic injuries in which HGF is up-regulated (Borowiak et al., 2004; Cramer et al., 2004; Huh et al., 2004). During hepatic injury, HGF is produced predominantly by stromal cells including stellate, endothelial, and Kupffer cells (Noji et al., 1990; Lalani et al., 2005). In contrast, c-Met is expressed mainly by hepatocytes

Received February 7, 2013. Accepted February 15, 2013.

Financial support was given to Radislav Sedláček by GACR (P305/10/2143), GACR (P303/10/2044), GAAV (IAA500520812), Academy of Sciences of the Czech Republic (RVO 68378050).

Corresponding author: Radislav Sedláček, Laboratory of Transgenic Models of Diseases, Institute of Molecular Genetics of the ASCR, v. v. i., Vídeňská 1083, 142 20 Prague 4, Czech Republic. Phone: (+420) 24106 3137; Fax: (+420) 22431 0955; e-mail: radislav.sedlacek@img.as.cz.

Abbreviations: ADAM – a disintegrin and metalloprotease, ALP – alkaline phosphatase, ALT – alanine aminotransferase, AST – aspartate transaminase, DDC – 3,5-diethoxycarbonyl-1,4-dihydroxycollidine, ELISA – enzyme-linked immunosorbent assay, GAPDH – glyceraldehyde-3-phosphate dehydrogenase, H&E – haematoxylin and eosin, HGF – hepatocyte growth factor, HSCs – hepatic stellate cells, MAPK – mitogen-activated protein kinase, MNs – mononuclear cells, PI3K – phosphatidylinositol 3-kinase, PMA – phorbol-12-myristate-13-acetate, PMNs – polymorphonuclear cells, qRT-PCR – quantitative reverse-transcription polymerase chain reaction, SDS – sodium dodecyl sulphate, sMet – soluble c-Met, SR – sirius red, TACE – TNF-α-converting enzyme, TNF-α – tumour necrosis factor α, TGF-β – transforming growth factor β, TIMP – tissue inhibitor of metalloproteinases.

(Schirmacher et al., 1992; Lalani et al., 2005). Thus, HGF/c-Met signalling is one of the examples of the heterotypic interaction between parenchymal and stromal cells in the liver. It is generally accepted that HGF expression is increased under necrotic and inflammatory liver conditions (Cramer et al., 2004), whereas the situation with c-Met is less clear as several reports describe both the down- and up-regulation of this receptor (Inoue et al., 2006; Takami et al., 2007; Marquardt et al., 2012).

It has been reported that c-Met signalling is regulated by several posttranslational mechanisms, among them internalization and proteolysis (Hammond et al., 2001, 2004). Proteolytic cleavage represents another mechanism for down-regulating c-Met signalling and involves the sequential proteolytic cleavages by two different protease systems. ADAMs release the extracellular domain generating a soluble N-terminal fragment. The membrane-bound cytoplasmic part then undergoes further proteolysis by γ-secretase, which yields a labile intracellular portion that is rapidly degraded in the proteasome (Prat et al., 1991; Foveau et al., 2009). The release of the cell surface protein ectodomain is termed shedding and is mainly attributed to members of the ADAM family. ADAM17 (also known as TACE, TNF-α-converting enzyme) and ADAM10 are the major sheddases (Pruessmeyer and Ludwig, 2009).

Shed c-Met circulates as a soluble N-terminal fragment, designated as sMet (Wajih et al., 2002; Petrelli et al., 2006; Schelter et al., 2010). This shedding of c-Met not only decreases the number of receptor molecules at the cell surface, but also creates a decoy moiety that binds to both HGF and membrane c-Met, inhibiting dimerization and transactivation of the native receptor (Zhang et al., 2004).

Although c-Met regulation and signalling is well described in the literature, the role of c-Met shedding during non-cancerous liver diseases is less known. As levels of soluble c-Met can be accurately assayed in blood serum (Zeng et al., 2009), we examined the relevance of sMet as a marker for hepatic damage and recovery. We show that, in addition to ADAM10, ADAM17 also sheds c-Met receptor and that sMet levels in serum tightly correlated with liver damage and recovery in a mouse model of DDC-induced hepatobiliary obstruction.

Material and Methods

Animal model of DDC-induced biliary fibrosis

Biliary fibrosis was induced as described (Fickert et al., 2007) by feeding 2-month-old male C57BL/6NCrl mice (Charles Rivers Laboratories, Wilmington, MA) weighing ~22 grams with a 0.1% DDC-supplemented diet (Sniff, Soest, Germany) for 2 weeks. A second group of animals were fed a DDC-supplemented diet for 2 weeks and then allowed to recover for 3, 7, and 14 days under a standard mouse diet to study c-Met levels during recovery from induced cholestasis. Age-matched C57BL/6NCrl males fed with regular chow (Rod18-A10, LASvendi, Soest, Germany) were used as controls. All animal studies were performed in accordance with European directive 86/609/EEC and were approved by the Czech Central Commission for Animal Welfare.

Serum analyses

Blood was obtained by retro-orbital bleed from anesthetized mice. Sera were analysed for ALT, AST, ALP, and total bilirubin levels using commercial kits (Roche Diagnostics, Prague, Czech Republic). The serum level of mouse TNF-α was measured by multiplex assay with a Bio-Plex mouse array (Bio-Rad Laboratories, Prague, Czech Republic) using the Bio-Plex 200 System (Bio-Rad Laboratories). The serum level of mouse sMet was assayed by enzyme-linked immunosorbent assay (ELISA) using an R&D Systems kit (R&D Systems, Minneapolis, MN) according to the manufacturer's instructions.

Quantitative Reverse-Transcription Polymerase Chain Reaction (qRT-PCR)

Total RNA was isolated from snap-frozen liver samples or cell cultures using TriReagent (Sigma-Aldrich, St. Louis, MO) according to the manufacturer's instructions. Specific primers were designed to amplify ~100 bp fragments of target gene transcripts using QuantPrime online software (Arvidsson et al., 2008). qRT-PCR was carried out directly from isolated RNA using the Kapa SYBR Fast One-Step qRT-PCR Kit (Kapa Biosystems, Boston, MA) and a LightCycler 480 (Roche, Mannheim, Germany). Reactions were performed in triplicates with the following conditions: 42 °C for 5 min, 95 °C for 3 min, followed by 40 cycles of 95 °C for 30 s, 60 °C for 30 s, and 72 °C for 30 s. The standard curve method was used to quantitate relative mRNA abundance. For normalization of the qRT-PCR data, glyceraldehyde-3-phosphate dehydrogenase (GAPDH) expression was used as the control and relative expression of the gene of interest was calculated by the 2-ΔΔCt method (Livak and Schmittgen, 2001). Primers used are listed in Table 1.

cDNA constructs and cloning

The human cDNA clone of full-length ADAM17 in the pCMV6-XL4 vector was obtained from OriGene (SC316426; OriGene Technologies, Rockville, MD). The human full-length ADAM10 cDNA was codon-optimized for human cell line expression using the OptimumGene design platform (Genscript, Piscataway, NJ), which employs a unique algorithm and proprietary codon usage table. Modifications for codon usage bias and GC content were made throughout the sequence in approximately 34.5 % of the DNA and codon-optimized ADAM10 was successfully assembled using overlapping PCR (Genscript). For the ectopic expression of untagged versions of ADAM17 and ADAM10, cDNA was PCR amplified from these plasmids and subcloned into the multiple cloning site 1 (MSC1) of the pVitro2-blasti

Table 1. Primer sequences for qRT-PCR

	forward (5‘-3‘)	reverse (5‘-3‘)
c-Met	TTCTGCTTGGCAACGAGAGCTG	GGGACCAACTGTGCATTTCAACG
ADAM17	AGCGTGAAGTGGCAGAACTT	GCCCCATCTGTGTTGATTCT
TNF-α	CCACCACGCTCTTCTGTCTA	AGGGTCTGGGCCATAGAACT
HGF	TGGCTTGGCATCCACGA	AGTTATCCAGGATTGCAGGTCGAG
ADAM10	AGCAACATCTGGGGACAAAC	TGGCCAGATTCAACAAAACA
TIMP1	ATGGAAAGCCTCTGTGGATATG	AAGCTGCAGGCACTGATGTG
TIMP3	CACGGAAGCCTCTGAAAGTC	TCCACAAAGTTGCACAGTCC
GAPDH	AACTTTGGCATTGTGGAAGG	GTCTTCTGGGTGGCAGTGAT

plasmid (InvivoGen, San Diego, CA). The TdTomato and EGFP coding sequences were then amplified from plasmids (pEGFP; Clontech and pRSET-B-tdTomato; kindly provided by Roger Tsien, University of California, San Diego, CA) and subcloned into MSC2 of either pVitro-ADAM17 or pVitro-ADAM10 vector to generate pVitro-ADAM17-TdTomato and pVitro-ADAM10--EGFP constructs encoding ADAMs and reporter proteins under the control of a composite ferritin promoter. All plasmids were verified by sequencing.

Shedding assay

Immortalized human liver hepatocellular carcinoma HepG2 cells and hepatic stellate cells (HSCs) LX2 (a model for partially activated HSCs (Xu et al., 2005); a kind gift of Scott Friedman, Mount Sinai, NY) were cultured in Dulbecco’s Modified Eagle’s Medium (Sigma-Aldrich), supplemented with 2% heat-inactivated foetal bovine serum (PAA Laboratories, Colbe, Germany), 10 mg/ml penicillin/streptomycin (PAA Laboratories). To obtain subconfluent cultures (~80 % confluence) for further experiments, cells were seeded at 2×10^3 cells/cm^2 in 6-well culture plates (Costar, Cambridge, MA). Transient transfections of HepG2 and LX2 cells were carried out using X-tremeGENE HP (Roche) according to the manufacturer’s instructions with 2 μg plasmid and a 1 : 3 (w/v) ratio of DNA to transfection reagent. The cells were incubated with the transfection complexes for 48 h and assayed after an additional 24 h. Overnight starved cells were either left untreated or exposed to 10 μmol/l metalloproteinase inhibitor TAPI-2 (EMD-Millipore, Billerica, MA) for 2 h prior to stimulation with 10 nmol/l phorbol-12-myristate-13-acetate (PMA; Sigma-Aldrich) for additional 24 h. Culture media were centrifuged at 12 000 × *g* for 15 min at 4 °C. Supernatants were analysed for sMet and TNF-α by colorimetric ELISA assays (R&D Systems) using an EnVision Multilabel Reader (PerkinElmer, Waltham, MA).

Immunoblotting

Total protein was isolated from cell cultures using TriReagent (Sigma-Aldrich) according to the manufacturer’s instructions. Protein precipitates were dissolved in 1% w/v sodium dodecyl sulphate (SDS) and stored at -80 °C. Protein concentration was determined using the BCA Protein Assay Kit (Thermo Scientific Pierce, Wilmington, DE). Proteins were separated in 10% SDS gels (25 μg per lane) and transferred to a nitrocellulose membrane (Whatman, Maidstone, UK). Immunoblots were probed with the following primary antibodies: anti-ADAM17 (1 : 1000; R&D Systems), anti-V5 epitope tag (1 : 1000; Cell Signaling Technology, Boston, MA), anti-ADAM10 (1 : 1000; Abcam, Cambridge, UK) and anti-GAPDH (1 : 50,000; Sigma-Aldrich). All secondary antibodies were peroxidase-conjugated: rabbit anti-goat and goat anti-rabbit (both 1 : 10,000; Sigma-Aldrich). Signals were detected by ECL plus Western Blotting Detection System (Cell Signaling Technology) and recorded with a Luminescent Image Analyzer (LAS-3000, Fujifilm Life Science, Düsseldorf, Germany).

Histology

Tissue samples were fixed in 4% neutral buffered formaldehyde for 24 h at 4 °C and processed in an automated tissue processor (Leica Microsystems, Leitz, Germany). Sections (3 μm) were stained with haematoxylin and eosin (H&E) staining. Sirius red (SR) staining was done by immersion in Fouchet’s reagent (Sigma-Aldrich) followed by incubation in celestine blue (Sigma-Aldrich), counterstaining with Harris haematoxylin. Then, the sections were incubated in SR solution (Sigma-Aldrich) for 20 min. Stained slides were dehydrated in ascending alcohol concentrations and mounted in Entellan® permanent mounting medium (Merck, Darmstadt, Germany). Analysis of the stained slides was performed using a Zeiss Axio Imager microscope (Zeiss Czech Republic, Prague, Czech Republic) equipped with polarization filter and Axiocam ERc5s digital camera. Representative images were captured at 20 × (H&E and SR) and 40 × (H&E) magnification and processed consecutively using the GIMP graphic editor version 2.8 (Free Software Foundation, Boston, MA). Scoring of SR staining was made semi-quantitatively by counting the number of SR-positive fibres in surface sections of the lobules, excluding the central vein. Fibre scoring was as follows: less than 5, negative (score 0); above 15, weakly positive (score 1); above 30, moderately positive (score 2), and uncountable, highly positive (score 3). At least 10 lobules per section were counted.

Statistical analysis

Statistical analyses were performed with GraphPad Prism software version 5.04 (GraphPad Software, San Diego CA). Results from independent experiments were analysed with two-tailed one-way ANOVA followed by

Student-Newman-Keuls post-hoc test. Data are presented as mean values; error bars in figures represent SEM; N values and statistical significance are specified in figure legends.

Results

To analyse the process of c-Met release from the surface of both, parenchymal and non-parenchymal cells, we used the hepatocellular HepG2 cells and LX2 cells transiently expressing either human ADAM17, or human ADAM10. LX2 cells were in addition transiently transfected with human c-Met, as their endogenous levels of HGF receptor are considerably lower. Transfected cells were analysed using immunoblotting for the ectopic expression of ADAM17, ADAM10, c-Met (Fig. 1A,B), and simultaneously also for released sMet and TNF-α, which is one of the main ADAM17 substrates.

Experiments showed that ADAM17, and to a lesser extent also previously reported ADAM10, causes shedding of c-Met, as its ectopic expression increased the amount of sMet in cell supernatants of HepG2 (Fig. 2A) and LX2 cells (Fig. 3A; compare mock and ADAM17 control and PMA stimulation). Moreover, the treatment with ADAM17-specific inhibitor TAPI-2 resulted in a significant reduction of sMet generation (Figs. 2A and 3A) in cells transfected with mock, c-Met, or ADAM17 but not in cells transfected with ADAM10 (Figs. 2A and 3A) in the cell lines.

The release of sMet and TNF-α into supernatants increased upon cell treatment with PMA irrespectively of whether the cells were transfected with c-Met or ADAM proteinases (Figs. 2A,B and 3A,B). The experiments clearly demonstrate ADAM17-mediated c-Met and TNF-α shedding, although the activity of ADAM17 towards TNF-α could be ascertained only through its response to the inhibitor TAPI-2 (Figs. 2A,B and 3A,B). The inhibition of shedding of c-Met by TAPI-2 was also obvious in untreated cells. However, the combination of PMA treatment and ectopic expression augmented the release of sMet, and thus the inhibition of c-Met shedding was more apparent (Figs. 2A and 3A). The ectopic expression of both ADAMs increased the release of soluble proteins in comparison to mock control (Figs. 2A,B and 3A,B) and this release was further augmented by PMA stimulation. However, since the experiments with transiently expressed ADAM proteinase detected endogenous sMet (i.e. not ectopically expressed), the remarkable growth of sMet release was detected only in LX2 cells and not in HepG2 cells. This is likely due to a different ratio of sheddases, mainly ADAM17, and the available cell-surface c-Met; shedding of endogenous c-Met reached its maximum in hepatocytes after the PMA treatment that activates both the endogenous and ectopically expressed ADAM17. Strikingly, TAPI-2 significantly reduced the amount of shed c-Met in supernatants of HepG2 and LX2 cells transfected with ADAM17, but no effect was seen for ADAM10 over-expressing

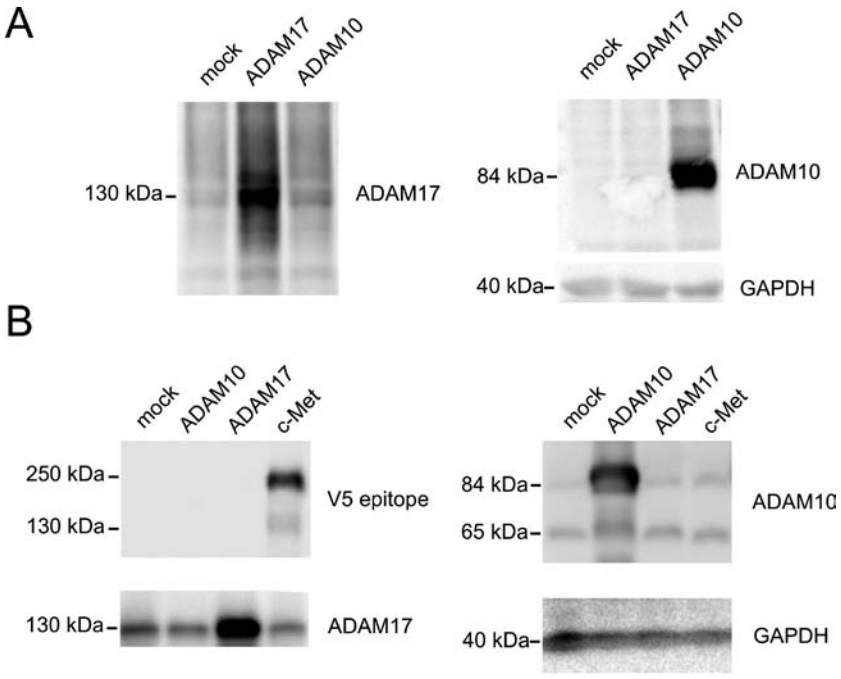

Fig. 1. Western blot analysis of HepG2 and LX2 cells transfected with plasmids encoding c-Met, ADAM17, ADAM10. **A,B** HepG2 (A) or LX2 (B) cells were transfected either with plasmids encoding c-Met, ADAM17, ADAM10, or with control empty vector (mock). Cell lysates from transfected cells were analysed by immunoblotting with anti-ADAM17, anti-ADAM10, and anti-V5 epitope antibodies. Equal amounts of proteins were loaded in each lane and protein bands were visualized as described in the Material and Methods section. GAPDH, loading control. Note, the air bubble in upper-right panel does not interfere with either transfer or visualization of assayed ADAM10.

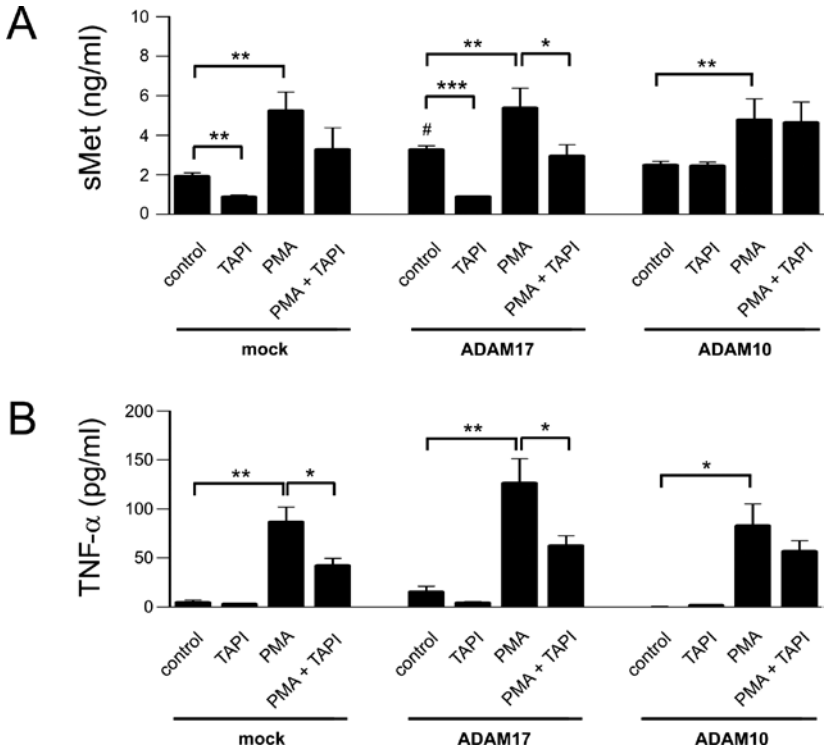

Fig. 2. c-Met is shed from hepatocellular HepG2 cells by ADAM17. **A,B** HepG2 cells were transfected either with plasmids encoding ADAM17, ADAM10, or with control empty vector (mock). Transfected cells were either treated with 10 nmol/l TAPI-2 2 h prior to 24-h incubation with 10 μmol/l PMA or left non-treated (control). Levels of human sMet (A) and TNF-α (B) in conditioned media were measured by ELISA.
Mean values ± SEM are shown (N = 3). *P < 0.05; **P < 0.01; ***P < 0.001; #P < 0.05 vs control/mock.

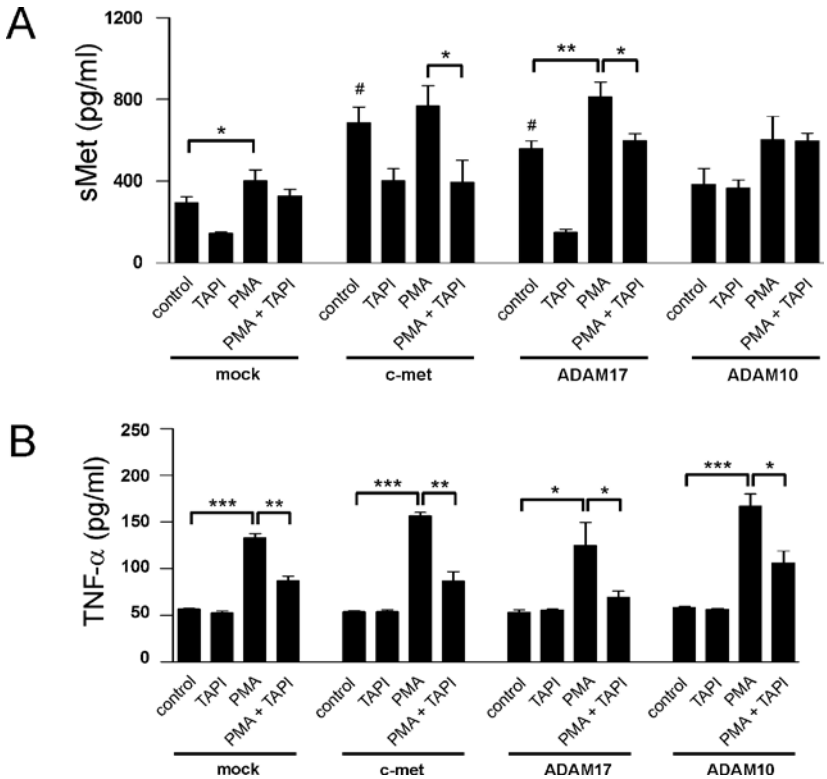

Fig. 3. c-Met is shed from the hepatic stellate cells LX2 by ADAM17 and ADAM10. **A,B** LX2 cells were transfected either with plasmids encoding c-Met, ADAM17, ADAM10, or with control empty vector (mock). Transfected cells were either treated with 10 nmol/l TAPI-2 2 h prior to 24-h incubation with 10 μmol/l PMA or left non-treated (control). Levels of human sMet (A) and TNF-α (B) in conditioned media were measured by ELISA.
Mean values ± SEM are shown (N = 3). *P < 0.05; **P < 0.01; ***P < 0.001; #P < 0.05 vs control/mock.

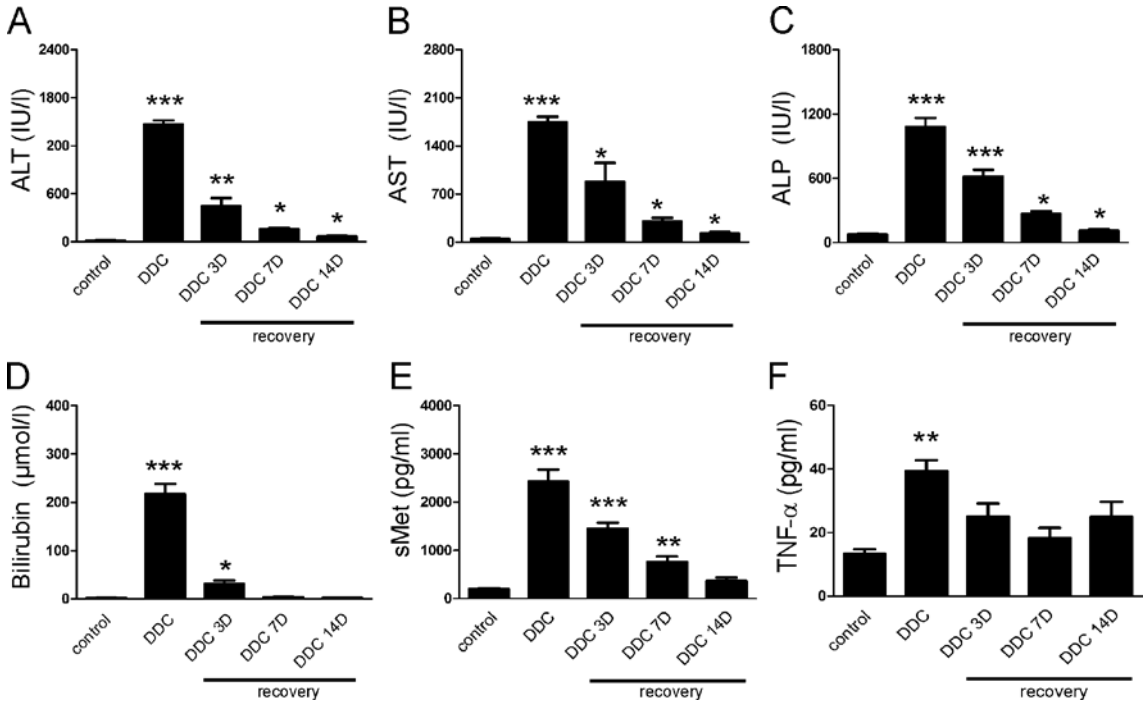

Fig. 4. Increased serum levels of sMet parallel increased levels of serum transaminases and bilirubin in a mouse model of DDC-induced acute cholestasis. **A-F** Biliary fibrosis was induced in C57BL/6NCrl mice by feeding with a DDC-supplemented diet for two weeks. Serum was collected from DDC-fed animals (DDC), animals allowed 3 (DDC 3D), 7 (DDC 7D), and 14 (DDC 14D) days of recovery on normal diet, and non-treated animals (control). Serum levels of ALT (A), AST (B), ALP (C), bilirubin (D), sMet (E) and TNF-α (F) were assessed as described in the text.
Mean values ± SEM are shown (N = 6). *P < 0.05; **P < 0.01; ***P < 0.001.

cells (Figs. 2A and 3A). Altogether, these data demonstrate that sMet is released mainly by ADAM17.

The release of sMet may represent an important control mechanism in regulating HGF/c-Met signalling in the liver and could thus reflect the level of liver damage and recovery. Therefore, we addressed the question whether sMet could serve as a biomarker to monitor liver disease development and recovery using a mouse model of acute cholestasis induced by DDC diet (Fickert et al., 2007). Increased serum levels of ALT, AST, ALP, and bilirubin are established markers of liver damage and their augmented levels were also observed in the serum of DDC-treated mice (Fig. 4A-D), suggesting the occurrence of hepatocellular damage. In the DDC model we observed that sMet levels were remarkably increased after two weeks of DDC diet compared to untreated animals and correlated well with the increase of ALT, AST, ALP, and bilirubin. These changes were also paralleled by augmented TNF-α levels, a well-known substrate of ADAM17. Furthermore, sMet levels gradually declined during the recovery phase of the DDC-induced cholestasis, although its level was still slightly elevated in comparison to untreated animals. The decline of sMet levels during recovery correlated with serum levels of all measured markers of hepatocellular injury. In contrast, the levels of soluble TNF-α (Fig. 4F), but not its mRNA levels (Fig. 5F), were still augmented during the whole recovery period, indicating likely ongoing inflammatory process. Thus, the serum levels of sMet reliably reflect progression and recovery from induced cholestasis and could be taken into consideration as a marker for hepatobiliar damage.

To distinguish whether the high levels of sMet in the model of mouse cholestasis was due to the proteolytic activity or due to the changes in c-Met or ADAM proteinase expression, the expression of HGF, TNF-α, tissue inhibitor of metalloproteinases (TIMP) 1 and 3 was examined at the mRNA level in liver samples of mice treated with DDC. Quantitative RT-PCR analysis revealed that the expression of c-Met was slightly elevated in the recovery phase (Fig. 5A) and this elevation lasted for the whole 14-day recovery period (see also Fig. 7). The expression of ADAM10 and ADAM17 was augmented after the two weeks of DDC diet and during early recovery phase, respectively (Fig. 5B,C). Then, their expression decreased to the levels observed in untreated controls. The mRNA level of TIMP1, the main matrix metalloproteinase inhibitor, which counteracts the proteolytic activity of matrix metalloproteinases during degradation of liver extracellular matrix (Hemmann et al., 2007), returned to the expression level observed prior to the damage at the end of the recovery period (Fig. 5F), while the expression of TIMP3, a main endogenous inhibitor of ADAM17, was not significantly changed (data not shown).

Mice treated for two weeks with DDC diet exhibited extensive hepatobiliary damage characterized by a number of bile plugs in the peritriad small bile ducts (Fig.

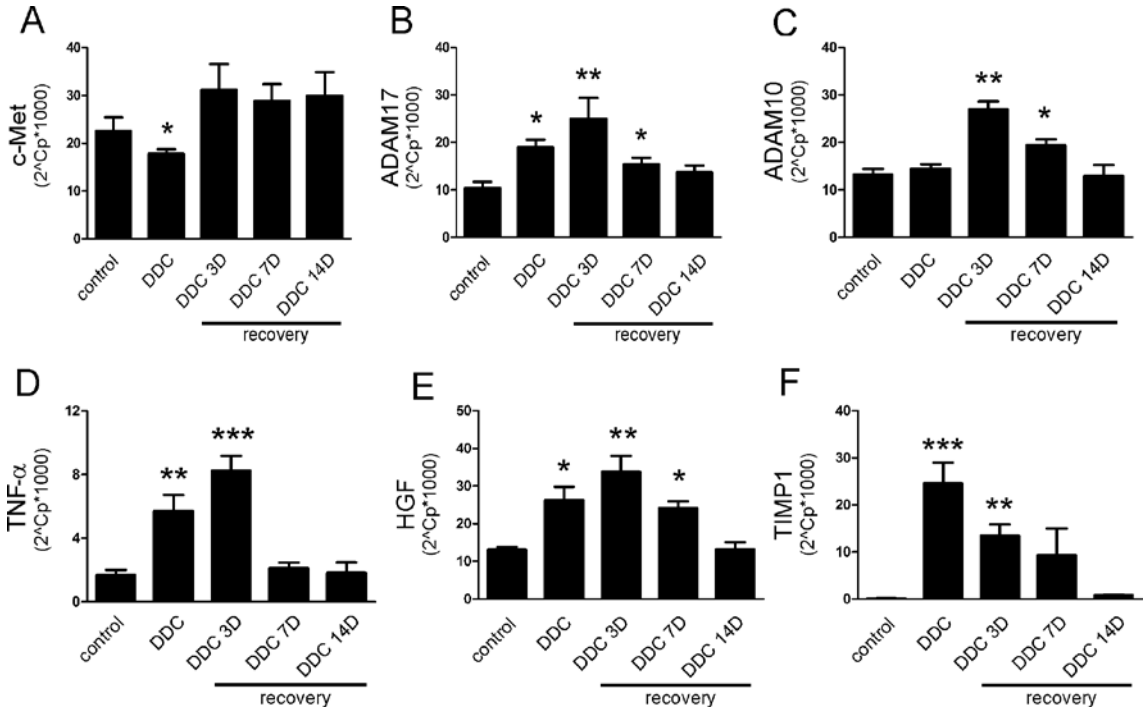

Fig. 5. mRNA levels of factors involved in DDC-induced acute cholestasis and c-Met regulation. **A-F** Liver samples were collected from DDC-fed animals (DDC), animals allowed 3 (DDC 3D), 7 (DDC 7D), and 14 (DDC 14D) days of recovery on normal diet, and non-treated animals (control), and mRNA was isolated and the relative expression levels of c-Met (A), ADAM17 (B), ADAM10 (C), TNF-α (D), HGF (E), TIMP1 (F), and TIMP3 (G) were followed by qRT-PCR. Expression of genes of interest was normalized to GAPDH and expressed as 2^Cp*1000 (for details see Material and Methods section). Mean values ± SEM are shown (N = 4). *P < 0.05; **P < 0.01; ***P < 0.001.

6E, arrows). In addition, analysis of H&E-stained liver slices showed marked infiltration with mononuclear (MNs) and polymorphonuclear (PMNs) inflammatory cells around the ducts, intraepithelial infiltration with PMNs (Fig. 6H, arrows), and interstitial infiltration of MNs containing bile debris in the periductal stroma (Fig. 6G, arrowheads). Occasional giant cells resembling Langhans-type cells were observed around the small bile ducts (Fig. 6F, asterisk). Intralobular, small but multiple, collagen deposits were frequently found using SR staining, suggesting development of early fibrosis (Fig. 6I). Altogether, these observations suggest development of acute cholangial inflammation due to bile duct obstruction and low-grade liver fibrosis.

In comparison to unchallenged animals, DDC-treated mice allowed to recover for three days exhibited lower amount of bile duct plugs (Fig. 6J), low-grade microvesicular hepatocyte steatosis (Fig. 6J, arrows). Also, the extent of periductal PMN infiltration (Fig. 6L, arrowheads) and the number of MNs containing phagocytosed bile debris localized in the periductal interstitium (Fig. 6K, arrow) were reduced. The SR staining showed a decreased number of collagen deposits in the liver lobules (Fig. 6M).

Liver from mice after seven days of recovery revealed residual periductal inflammation manifested by occasional occurrence of MNs with bile debris found in the periductal interstitium (Fig. 6P, arrowhead). Liver parenchyma contained numerous polyploid hepatocytes with evident nuclear indentations, suggesting possible endomitosis (Fig. 6O, arrow).

Mice recovered for 14 days showed only a small number of bile debris-containing MNs (Fig 6R, arrows). No residual inflammatory infiltrate around the bile ducts (Fig. 6T, asterisk) was found, although numerous binucleated hepatocytes were seen in the peritriad regions and close to the central veins (Fig. 6S, arrows), suggesting ongoing hepatocyte proliferation.

Discussion

HGF and its specific receptor, c-Met, play a pivotal role in liver development and regeneration, particularly in response to acute and chronic injuries (Trusolino et al., 2010). Subsequent to hepatic injury, the production of HGF is rapidly up-regulated. The resultant increase in c-Met signalling provides not only a strong mitogenic and anti-apoptotic stimulus to hepatocytes, but also antagonizes transforming growth factor β (TGF-β)-dependent profibrogenic responses (Ueki et al., 1999). It is well established that acute HGF stimulation leads to down-regulation of the receptor by internalization (Hammond et al., 2001, 2004), which results either in recycling of the receptor or degradation via the lysosomal pathway (Teis and Huber, 2003). Generally, the rapid removal of the receptor from the cell surface and

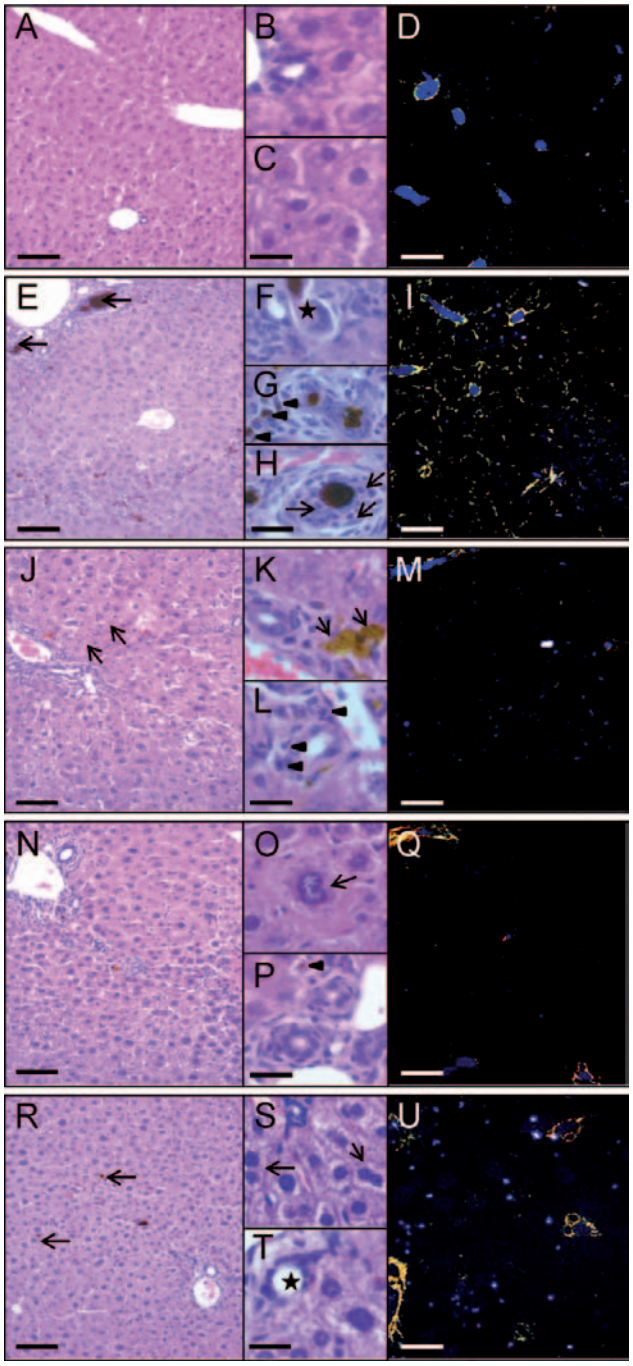

Fig. 6. Histological evaluation of liver injury correlates with serum levels of c-Met and other markers of hepatobiliary injury and recovery. Tissue sections of liver isolated from non-treated animals (A-D), DDC-fed animals (E-I), and animals allowed 3 (J-M), 7 (N-Q), and 14 (R-U) days of recovery on normal diet were stained with H&E (A-C, E-H, J-L, N-P, R-T) or SR (D,I,M,Q,U). **A-D** Control animals exhibited no inflammatory cholangitis and hepatocyte dystrophy. **E-I** Mice after DDC treatment showed massive plugs in the small peritriad ducts (E, arrows) and inflammatory infiltrate composed of mononuclear (MNs) and polymorphonuclear (PMNs) cells (G,H). The MNs infiltrated the periductal connective tissue (G, arrowheads), while the PMNs infiltrated the epithelium of the plugged bile ducts (H, arrows). SR staining revealed a low level of lobular fibrosis (I). **J-M** Hepatocytes exhibited vacuolar dystrophy especially around the triads (J, arrows). Reduced number of PMNs can be seen (J), not infiltrating the ducts but in the periductal connective tissue (L, arrowheads). The MN number is lowered but the amount of contained bile debris is higher (K, arrows). SR birefringence did not reveal collagen deposits (M). **N-Q** Seven days of recovery; no sign of PMN infiltration around bile ducts, remaining MNs with bile debris (P, arrowhead). Numerous giant hepatocytes were found in the stage of endomitosis (O, arrow); no fibrosis could be seen in the tissue (Q). **R-U** Fourteen days of recovery; there is a small amount of MNs (R, arrows), no detectable bile plugs in the ducts (T*), and numerous binucleated hepatocytes (S, arrows) around the triad regions. No collagen deposits were detected in SR staining.
Scale bars 100 µm (A,E,J,N,R), 50 µm (B,C,F,G,H,K,L,O, P,S,T), and 200 µm (D,I,M,Q,U).

its following degradation is believed to provide a mechanism for preventing the sustained activation of downstream signalling, as this could potentially lead to transformation.

Further modulation of c-Met signalling occurs via shedding of its ectodomain, a process mediated by members of the ADAM family and involving subsequent γ-secretase proteolysis (Foveau et al., 2009). The ADAM family of metalloproteinases, recognized as the major proteinase family involved in protein ectodomain release (shedding), plays a pivotal role in the regulation of many processes as they mediate both pro-damage/pro-inflammatory responses as well as recovery and regeneration (Huovila et al., 2005; Hemmann et al., 2007; Scheller et al., 2011). Although previous investigations are ambiguous about c-Met release by ADAM-mediated proteolysis (Wajih et al., 2002; Petrelli et al., 2006; Schelter et al., 2010), our findings support the involvement of both ADAM17 and ADAM10. Previous studies implicated ADAM10 in c-Met shedding in mouse fibroblasts (Kopitz et al., 2007), although these results were not confirmed in epithelial cells (Foveau et al., 2009). A clearer picture about the involvement of ADAM10 and ADAM17 in c-Met shedding was shown in the study analysing sMet generation in placenta during preeclampsia (Yang et al., 2012). Our work is in line with this study and shows that c-Met in parenchymal and non-parenchymal cells of the liver is shed by both ADAMs and that ADAM17 appears to be the main sheddase, especially after activation of cells with PMA.

To elucidate which of the two ADAM proteinases is involved in c-Met shedding in liver cells, we examined generation of the soluble form of c-Met using HepG2 and LX2 cell lines ectopically expressing either ADAM proteinases or c-Met receptor. We showed that besides ADAM10 (Schelter et al., 2010), ADAM17 also mediates the shedding of c-Met, as the ectopic expression of ADAM17 increased the amount of sMet in cell supernatants. The release of c-Met (as well as TNF-α) was further augmented by PMA, while treating the cells with ADAM17-specific inhibitor TAPI-2 led to reduction of the sMet amount. As the inhibition of c-Met cleavage by TAPI-2 was only partial, it is likely that also other proteinases (including ADAM10) contribute to the shedding. Differential involvement of ADAM10 and ADAM17 in shedding c-Met in various cell populations in the liver could thus provide a molecular basis for the discrete effects of c-Met signalling in HSCs and hepatocytes. The loss of hepatocyte c-Met signalling mediates excessive activation of HSCs with consequent aggravation of inflammation and liver fibrosis (Marquardt et al., 2012). Administration of HGF was shown to reverse fibrosis and decrease hepatocyte apoptosis in parallel with increased apoptosis of HSCs (Matsuda et al., 1995; Kim et al., 2005). Our results indicating that both ADAM17 and ADAM10 can shed c-Met from the cell surface of hepatocytes and hepatic stellate cells suggests the intriguing possibility of another level of HGF--TGF-β1 crosstalk. TGF-β1-dependent up-regulation of ADAM17 mRNA and protein expression was recently shown in glioma cells (Lu et al., 2011). This correlates well with our data showing increased expression of both ADAM17 and ADAM10 in TGF-β1-stimulated LX2 cells (data not shown). It is conceivable that activation of HSCs by TGF-β1 leads to the up-regulation of sheddases, which by decreasing c-Met receptor availability would promote acceleration of liver fibrosis.

To reveal whether the sMet level in the serum is useful as an additional indicator of liver injury and recovery, we compared the expression of HGF/c-Met, ADAM10/17 with the levels in a murine model of DDC-induced hepatic injury which also allows studying the recovery phase. Using this model we show that the serum levels of sMet strongly correlated with the increase of serum AST, ALT, ALP, and bilirubin during the acute phase and mirrored histological measures of the severity of hepatobilliary injury, inflammation, and consecutive hepatocyte repair. Although changes in sMet generation are not used as a diagnostic tool, there is a report comparing plasma levels of sMet in healthy pregnant women with those suffering from severe preeclampsia. Preeclampsia was shown to be associated with significantly lower sMet levels (Zeng et al., 2009). Moreover, this study also documented sMet as a potential prognostic marker, revealing a significant correlation between the plasma sMet level and the potential to develop preeclampsia. Nevertheless, these observations have not been associated with any liver damage or dysfunction.

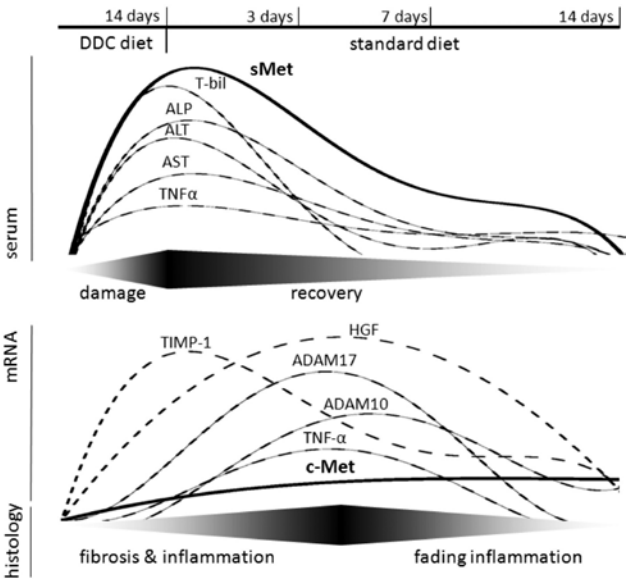

Fig. 7. Schematized expression profiles of biochemical markers of liver damage. ADAM proteinases, HGF/c-Met and their correlation with serum sMet levels in mice with DDC-induced biliary fibrosis. The lower graph shows mRNA expression data of various gene markers in the liver (see also Fig. 5); the upper graph shows serum levels of important biochemical markers in the indicated period of DDC treatment (see also Fig. 3) and their correlation with major histological changes (see also Fig. 6).

In the model of DDC-induced hepatobilliary damage, the expression of c-Met is elevated in the recovery phase, even though the serum level of sMet gradually declines. The decline of the sMet amount correlates well with liver recovery (Fig. 7). The peak of released sMet in the serum also correlates with an increase of ADAM17 expression in the liver, although its expression peaks later, at the beginning of the recovery phase. The increase in ADAM10 expression is delayed relative to that of ADAM17. However, the expression of both ADAMs reached its highest value at the same time. Moreover, as the expression of TIMP3, the main inhibitor of ADAM17, remained largely unchanged, the increased serum levels of sMet in the mouse model of acute cholestasis could be mainly attributed to the elevated expression of both ADAM proteinases and their increased proteolytic activity. This may suggest that ADAM17 is the primary mediator of c-Met shedding under acute pathogenesis or inflammatory conditions, while ADAM10, which declines more slowly than ADAM17 (Fig. 7), may be responsible for sMet production in the later recovery phase. The generation of sMet could also be supported by elevated expression in recovery phase, which lasted for the whole 14-day recovery period (Fig. 7). This finding is consistent with the previous observation that during acute liver damage the expression level of HGF but not c-Met regulates proliferation and liver repair (Corpechot et al., 2002). Similarly to previously published results (Zarnegar et al., 1991; Diehl, 2000; Morio et al., 2001; Lalani et al., 2005), the mRNA levels

of HGF and TNF-α in the DDC-induced mouse cholestasis model were elevated in both the acute and early recovery phase. Nevertheless, it is unclear how high levels of sMet in the serum are achieved if c-Met expression is up-regulated only moderately. As the generation of sMet did not fully correlate with the expression of ADAM proteases, the question arises whether another protease(s) is involved in c-Met shedding in the initial acute phase of injury as well as in last phase of recovery, when the expression levels of both ADAM10 and ADAM17 are back to the values observed prior to the liver damage.

In this report, we show that the levels of sMet in the serum mirror hepatic conditions (hepatic damage and recovery) and that this release is dependent on the proteolytic activity of the two sheddases, ADAM10 and ADAM17. These proteinases appear to be responsible for the release of sMet during acute liver damage and inflammation, although ADAM17 appears to be the main sheddase after cell activation. Since the amount of sMet in serum correlates very well with the histopathology of liver as well as aminotransferase markers of liver damage, the amount of sMet might be a meaningful endogenous biomarker of hepatocyte damage and especially liver regeneration.

Acknowledgement

We thank S. Friedman and R. Tsien for generously provided material and A. Juhasz, M. Pickova and L. Sarnova for their outstanding technical assistance. We are also grateful to T. Epp for critical reading of the manuscript.

References

Arvidsson, S., Kwasniewski, M., Riano-Pachon, D. M., Mueller-Roeber, B. (2008) QuantPrime – a flexible tool for reliable high-throughput primer design for quantitative PCR. *BMC Bioinformatics* **9**, 465.

Birchmeier, C., Birchmeier, W., Gherardi, E.,Vande Woude, G. F. (2003) Met, metastasis, motility and more. *Nat. Rev. Mol. Cell. Biol.* **4**, 915-925.

Borowiak, M., Garratt, A. N., Wustefeld, T., Strehle, M., Trautwein, C., Birchmeier, C. (2004) Met provides essential signals for liver regeneration. *Proc. Natl. Acad. Sci. USA* **101**, 10608-10613.

Comoglio, P. M. (2001) Pathway specificity for Met signalling. *Nat. Cell Biol.* **3**, E161-162.

Corpechot, C., Barbu, V., Wendum, D., Chignard, N., Housset, C., Poupon, R., Rosmorduc, O. (2002). Hepatocyte growth factor and c-Met inhibition by hepatic cell hypoxia: a potential mechanism for liver regeneration failure in experimental cirrhosis. *Am. J. Pathol.* **160**, 613-620.

Cramer, T., Schuppan, D., Bauer, M., Pfander, D., Neuhaus, P., Herbst, H. (2004) Hepatocyte growth factor and c-Met expression in rat and human liver fibrosis. *Liver Int.* **24**, 335-344.

Diehl, A. M. (2000) Cytokine regulation of liver injury and repair. *Immunol. Rev.* **174**, 160-171.

Fickert, P., Stoger, U., Fuchsbichler, A., Moustafa, T., Marschall, H. U., Weiglein, A. H., Tsybrovskyy, O., Jaeschke, H., Zatloukal, K., Denk, H., Trauner, M. (2007) A new xenobiotic-induced mouse model of sclerosing cholangitis and biliary fibrosis. *Am. J. Pathol.* **171**, 525-536.

Foveau, B., Ancot, F., Leroy, C., Petrelli, A., Reiss, K., Vingtdeux, V., Giordano, S., Fafeur, V., Tulasne, D. (2009) Down-regulation of the met receptor tyrosine kinase by presenilin-dependent regulated intramembrane proteolysis. *Mol. Biol. Cell* **20**, 2495-2507.

Giordano, S., Di Renzo, M. F., Ferracini, R., Chiado-Piat, L., Comoglio, P. M. (1988) p145, a protein with associated tyrosine kinase activity in a human gastric carcinoma cell line. *Mol. Cell. Biol.* **8**, 3510-3517.

Hammond, D. E., Urbe, S., Vande Woude, G. F., Clague, M. J. (2001) Down-regulation of MET, the receptor for hepatocyte growth factor. *Oncogene* **20**, 2761-2770.

Hammond, D. E., Carter, S., Clague, M. J. (2004) Met receptor dynamics and signalling. *Curr. Top. Microbiol. Immunol.* **286**, 21-44.

Hemmann, S., Graf, J., Roderfeld, M., Roeb, E. (2007) Expression of MMPs and TIMPs in liver fibrosis – a systematic review with special emphasis on anti-fibrotic strategies. *J. Hepatol.* **46**, 955-975.

Huh, C. G., Factor, V. M., Sanchez, A., Uchida, K., Conner, E. A., Thorgeirsson, S. S. (2004) Hepatocyte growth factor/c-met signaling pathway is required for efficient liver regeneration and repair. *Proc. Natl. Acad. Sci. USA* **101**, 4477-4482.

Huovila, A. P., Turner, A. J., Pelto-Huikko, M., Karkkainen, I., Ortiz, R. M. (2005) Shedding light on ADAM metalloproteinases. *Trends Biochem. Sci.* **30**, 413-422.

Inoue, H., Yokoyama, F., Kita, Y., Yoshiji, H., Tsujimoto, T., Deguchi, A., Nakai, S., Morishita, A., Uchida, N., Masaki, T., Watanabe, S., Kuriyama, S. (2006) Relationship between the proliferative capability of hepatocytes and the intrahepatic expression of hepatocyte growth factor and c-Met in the course of cirrhosis development in rats. *Int. J. Mol. Med.* **17**, 857-864.

Kim, W. H., Matsumoto, K., Bessho, K., Nakamura, T. (2005) Growth inhibition and apoptosis in liver myofibroblasts promoted by hepatocyte growth factor leads to resolution from liver cirrhosis. *Am. J. Pathol.* **166**, 1017-1028.

Kopitz, C., Gerg, M., Bandapalli, O. R., Ister, D., Pennington, C. J., Hauser, S., Flechsig, C., Krell, H. W., Antolovic, D., Brew, K., Nagase, H., Stangl, M., von Weyhern, C. W., Brucher, B. L., Brand, K., Coussens, L. M., Edwards, D. R., Kruger, A. (2007) Tissue inhibitor of metalloproteinases-1 promotes liver metastasis by induction of hepatocyte growth factor signaling. *Cancer Res.* **67**, 8615-8623.

Lalani el-N., Poulsom, R., Stamp, G., Fogt, F., Thomas, P., Nanji, A. A. (2005) Expression of hepatocyte growth factor and its receptor c-met, correlates with severity of pathological injury in experimental alcoholic liver disease. *Int. J. Mol. Med.* **15**, 811-817.

Livak, K. J., Schmittgen, T. D. (2001) Analysis of relative gene expression data using real-time quantitative PCR and the 2(-Δ Δ C(T)) Method. *Methods* **25**, 402-408.

Lu, Y., Jiang, F., Zheng, X., Katakowski, M., Buller, B., To, S. S., Chopp, M. (2011) TGF-β1 promotes motility and inva-

siveness of glioma cells through activation of ADAM17. *Oncol. Rep.* **25**, 1329-1335.

Ma, P. C., Maulik, G., Christensen, J., Salgia, R. (2003) c-Met: structure, functions and potential for therapeutic inhibition. *Cancer Metastasis Rev.* **22**, 309-325.

Marquardt, J. U., Seo, D., Gomez-Quiroz, L. E., Uchida, K., Gillen, M. C., Kitade, M., Kaposi-Novak, P., Conner, E. A., Factor, V. M., Thorgeirsson, S. S. (2012) Loss of c-Met accelerates development of liver fibrosis in response to CCl(4) exposure through deregulation of multiple molecular pathways. *Biochim. Biophys. Acta* **1822**, 942-951.

Matsuda, Y., Matsumoto, K., Ichida, T., Nakamura, T. (1995) Hepatocyte growth factor suppresses the onset of liver cirrhosis and abrogates lethal hepatic dysfunction in rats. *J. Biochem.* **118**, 643-649.

Morio, L. A., Chiu, H., Sprowles, K. A., Zhou, P., Heck, D. E., Gordon, M. K., Laskin, D. L. (2001) Distinct roles of tumor necrosis factor-α and nitric oxide in acute liver injury induced by carbon tetrachloride in mice. *Toxicol. Appl. Pharmacol.* **172**, 44-51.

Noji, S., Tashiro, K., Koyama, E., Nohno, T., Ohyama, K., Taniguchi, S., Nakamura, T. (1990) Expression of hepatocyte growth factor gene in endothelial and Kupffer cells of damaged rat livers, as revealed by in situ hybridization. *Biochem. Biophys. Res. Commun.* **173**, 42-47.

Petrelli, A., Circosta, P., Granziero, L., Mazzone, M., Pisacane, A., Fenoglio, S., Comoglio, P. M., Giordano, S. (2006) Ab-induced ectodomain shedding mediates hepatocyte growth factor receptor down-regulation and hampers biological activity. *Proc. Natl. Acad. Sci. USA* **103**, 5090-5095.

Prat, M., Crepaldi, T., Gandino, L., Giordano, S., Longati, P., Comoglio, P. (1991) C-terminal truncated forms of Met, the hepatocyte growth factor receptor. *Mol. Cell. Biol.* **11**, 5954-5962.

Pruessmeyer, J., Ludwig, A. (2009) The good, the bad and the ugly substrates for ADAM10 and ADAM17 in brain pathology, inflammation and cancer. *Semin. Cell. Dev. Biol.* **20**, 164-174.

Scheller, J., Chalaris, A., Garbers, C., Rose-John, S. (2011) ADAM17: a molecular switch to control inflammation and tissue regeneration. *Trends Immunol.* **32**, 380-387.

Schelter, F., Kobuch, J., Moss, M. L., Becherer, J. D., Comoglio, P. M., Boccaccio, C., Kruger, A. (2010) A disintegrin and metalloproteinase-10 (ADAM-10) mediates DN30 antibody-induced shedding of the met surface receptor. *J. Biol. Chem.* **285**, 26335-26340.

Schirmacher, P., Geerts, A., Pietrangelo, A., Dienes, H. P., Rogler, C. E. (1992) Hepatocyte growth factor/hepatopoietin A is expressed in fat-storing cells from rat liver but not myofibroblast-like cells derived from fat-storing cells. *Hepatology* **15**, 5-11.

Takami, T., Kaposi-Novak, P., Uchida, K., Gomez-Quiroz, L. E., Conner, E. A., Factor, V. M., Thorgeirsson, S. S. (2007) Loss of hepatocyte growth factor/c-Met signaling pathway accelerates early stages of N-nitrosodiethylamine induced hepatocarcinogenesis. *Cancer Res.* **67**, 9844-9851.

Teis, D., Huber, L. A. (2003) The odd couple: signal transduction and endocytosis. *Cell. Mol. Life Sci.* **60**, 2020-2033.

Trusolino, L., Bertotti, A., Comoglio, P. M. (2010) MET signalling: principles and functions in development, organ regeneration and cancer. *Nat. Rev. Mol. Cell. Biol.* **11**, 834-848.

Uehara, Y., Minowa, O., Mori, C., Shiota, K., Kuno, J., Noda, T., Kitamura, N. (1995) Placental defect and embryonic lethality in mice lacking hepatocyte growth factor/scatter factor. *Nature* **373**, 702-705.

Ueki, T., Kaneda, Y., Tsutsui, H., Nakanishi, K., Sawa, Y., Morishita, R., Matsumoto, K., Nakamura, T., Takahashi, H., Okamoto, E., Fujimoto J. (1999) Hepatocyte growth factor gene therapy of liver cirrhosis in rats. *Nat. Med.* **5**, 226-230.

Wajih, N., Walter, J., Sane, D. C. (2002) Vascular origin of a soluble truncated form of the hepatocyte growth factor receptor (c-met). *Circ. Res.* **90**, 46-52.

Xu, L., Hui, A. Y., Albanis, E., Arthur, M. J., O'Byrne, S. M., Blaner, W. S., Mukherjee, P., Friedman, S. L., Eng, F. J. (2005) Human hepatic stellate cell lines, LX-1 and LX-2: new tools for analysis of hepatic fibrosis. *Gut* **54**, 142-151.

Yang, Y., Wang, Y., Zeng, X., Ma, X. J., Zhao, Y., Qiao, J., Cao, B., Li, Y. X., Ji, L., Wang, Y. L. (2012) Self-control of HGF regulation on human trophoblast cell invasion via enhancing c-Met receptor shedding by ADAM10 and ADAM17. *J. Clin. Endocrinol. Metab.* **97**, E1390-1401.

Zarnegar, R., DeFrances, M. C., Kost, D. P., Lindroos, P., Michalopoulos, G. K. (1991). Expression of hepatocyte growth factor mRNA in regenerating rat liver after partial hepatectomy. *Biochem. Biophys. Res. Commun.* **177**, 559-565.

Zeng, X., Sun, Y., Yang, H. X., Li, D., Li, Y. X., Liao, Q. P., Wang, Y. L. (2009) Plasma level of soluble c-Met is tightly associated with the clinical risk of preeclampsia. *Am. J. Obstet. Gynecol.* **201**, 618.e1-7.

Zhang, Y. W., Graveel, C., Shinomiya, N., Vande Woude, G. F. (2004) Met decoys: will cancer take the bait? *Cancer Cell* **6**, 5-6.